ELSEVIER

Biophysical Chemistry 114 (2005) 191–197

Biophysical Chemistry

http://www.elsevier.com/locate/biophyschem

Prediction of the mutation-induced change in thermodynamic stabilities of membrane proteins from free energy simulations

Hwangseo Park*, Sangyoub Lee*

School of Chemistry and Molecular Engineering, Seoul National University, Seoul 151-747, Korea

Received 8 October 2004; received in revised form 2 December 2004; accepted 3 December 2004
Available online 22 December 2004

Abstract

Comparative protein structure modeling and free energy perturbation simulation have been applied in a consecutive manner to investigate the mutation-induced stabilization of membrane proteins (MPs) in aqueous solution without knowledge of their three-dimensional structures. The calculated difference in protein solvation free energy between the wild type and a mutant compares well with their relative thermodynamic stabilities in solution. For monomeric MPs, a mutant reveals a higher stability than the wild type if the calculated solvation free energy indicates a favorable change. On the contrary, for oligomeric MPs the stability of a mutant increases as the solvation free energy of a mutated monomer becomes less favorable, indicating that the oligomeric MP mutant would be stabilized in solution due to the reduced desolvation cost for oligomerization. The present computational strategy is expected to find its way as a useful tool for assessing the relative stability of a mutant MP with respect to its wild type in solution.

Keywords: Membrane proteins; Protein engineering; Solvation free energy; Molecular dynamics; Free energy simulation

1. Introduction

Although 25% to 30% of the proteins coded by the human genome are embedded in membranes, only about 2% of the known protein structures belong to the category of membrane proteins (MPs) [1]. This disparity in structural information stems from the instability of MPs in aqueous solution due to the possession of large hydrophobic patches on their surfaces. Nevertheless, considering the fundamental biological functions of MPs and their importance as drug targets, the development of methods for overcoming such a technical barrier in the structural determination of MPs represents the next frontier of structural genomics [2].

One way to maintain the MPs stable in aqueous solutions is to use detergent molecules that equilibrate between a monolayer covering the transmembrane surface of the protein and protein-free micelles [3]. However, the detergents often inhibit the crystallization of an MP in its active form, and the size of MP-detergent mixed micelles may be too large for NMR experiments [4]. An alternative way is to identify mutations that can enhance the stability of MPs in solution without involving loss of activity and significant structural change [5]. Although such mutations have been found in several MPs [6–10], most of them have been identified from randomly generated mutant libraries in which more than 90% of mutant proteins exhibited decreased stability. Therefore, researchers in structural biology are in urgent need of a rational engineering method for finding mutant MPs with the desired physical characteristics.

In this study, we propose to use comparative protein structure modeling and free energy perturbation (FEP) calculation in a consecutive way for predicting the stability-enhancing point mutations of MPs. Based on this method, we calculate the solvation free energy (SFE) differences between the wild type (WT) and mutants of

* Corresponding authors. Tel.: +82 2 875 4887; fax: +82 2 889 1568.
E-mail addresses: hwangseo@snu.ac.kr (H. Park), sangyoub@snu.ac.kr (S. Lee).

0301-4622/$ - see front matter © 2004 Elsevier B.V. All rights reserved.
doi:10.1016/j.bpc.2004.12.006

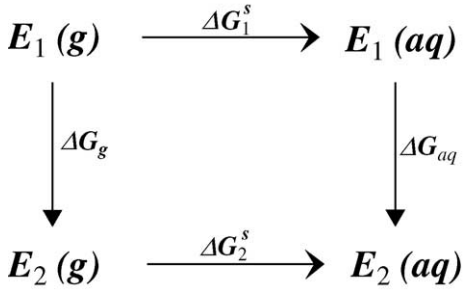

Fig. 1. Thermodynamic cycle used in calculating the difference in solvation free energies ($\Delta\Delta G_{sol}$) between the WT (E_1) and a mutant protein (E_2).

bacteriorhodopsin [11], OmpF porin [12], M13 coat protein [13], and lactose permease [14] in the monomeric states. Although the X-ray structures of these proteins have already been reported, we use the homology-modeled structures because we aim to propose a computational method for predicting the stability-enhancing point mutations in the membrane proteins for which 3D structures are unknown due to the instability in solution. The results will then be compared with the experimental thermodynamic stabilities to assess the predictive power of our computational strategy.

2. Computational methods

The peptide sequences of the targets (bacteriorhodopsin, OmpF porin, and M13 coat protein with accession numbers P02945, P02931, and P03617, respectively) and their respective templates (archaerhodopsin 1, phosphoporin, and IF1 coat protein with accession numbers P19585, P02932, and P03619, respectively) were retrieved from the SWISS-PROT protein sequence data bank (http://us.expasy.org/sprot). Sequence alignments between the targets and the templates were then derived with the CLUSTAL W package [15]. Based on these sequence alignments and X-ray structures of archaerhodopsin 1 [16], phosphoporin [17], and IF1 coat protein [13] with PDB ID's 1UAZ, 1PHO, and 1IFK, respectively, the 3D structures of bacteriorhodopsin, OmpF porin, and M13 coat protein were constructed using the MODELLER program of version 6v2 [18].

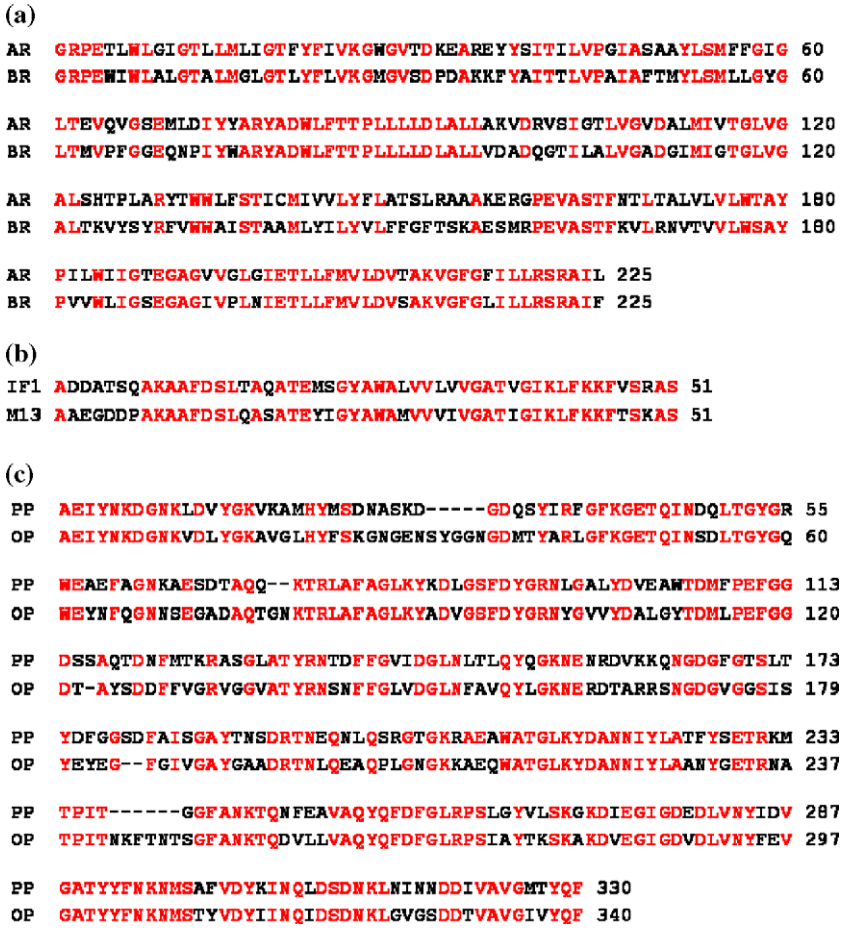

Fig. 2. Sequence alignments (a) between archaerhodopsin 1 (AR) and bacteriorhodopsin (BR), (b) between IF1 and M13 coat proteins, and (c) between phosphoporin (PP) and OmpF porin (OP).

In order to calculate the SFE change for a given point mutation, we employed a simple thermodynamic cycle as depicted in Fig. 1. Since the free energy is a state function, the sum of all free energy changes in a thermodynamic cycle is zero. Therefore, the relative change in SFE ($\Delta\Delta G_{sol}$) can be expressed as

$$\Delta\Delta G_{sol} \equiv \Delta G_2^s - \Delta G_1^s = \Delta G_{aq} - \Delta G_g \quad (1)$$

where ΔG_1^s and ΔG_2^s refer to the SFEs of the WT (E_1) and mutant protein (E_2), respectively, and ΔG_g and ΔG_{aq} to the free energy changes associated with the virtual transformations of E_1 into E_2 in the gas phase and in aqueous solution, respectively. We obtained $\Delta\Delta G_{sol}$ by FEP calculations of ΔG_g and ΔG_{aq} from independent molecular dynamics simulations in the gas phase and in aqueous solution with explicit solvent model.

To determine $\Delta\Delta G_{sol}$ between E_1 (initial state, WT) and E_2 (final state, mutant) based on the thermodynamic cycle depicted in Fig. 1, the free energy changes in transforming E_1 into E_2 should be calculated both in the gas phase (ΔG_g) and in aqueous solution (ΔG_{aq}). We computed them by perturbing the Hamiltonian of E_1 into E_2. This was accomplished through a parametrization of terms comprising the interaction potentials of the system with a change of state variable (λ), which maps onto initial and final states when λ is 0 and 1, respectively.

Molecular dynamics simulations of the four MP monomers were carried out using AMBER 7 [19] with the force field reported by Cornell et al. [20]. Each protein molecule was immersed in a rectangular box containing TIP3P [21] water molecules. After 1000 cycles of energy minimization, we equilibrated the systems beginning with 20 ps equilibration dynamics of the solvent molecules at 300 K. The next step involved equilibration of the solute with a fixed configuration of solvent molecules for 5 ps at 10, 50, 100, 150, 200, 250, and 300 K. Then, the equilibration dynamics of the entire system were performed at 300 K for 20 ps. The same procedure was used in the equilibration dynamics for protein molecules in the gas phase.

Following the equilibration dynamics, we performed 315 ps of perturbation in each direction for a given point mutation. Each perturbation consisted of 21 windows with 5 ps of equilibration and 10 ps of data collection. In this molecular dynamics-based FEP calculation, a periodic boundary condition was employed in the NPT ensemble at 300 K and 1 atm. The SHAKE algorithm was applied to fix all bond lengths involving hydrogen atoms [22]. We used a time step of 1 fs and a nonbonded-interaction cut-off radius

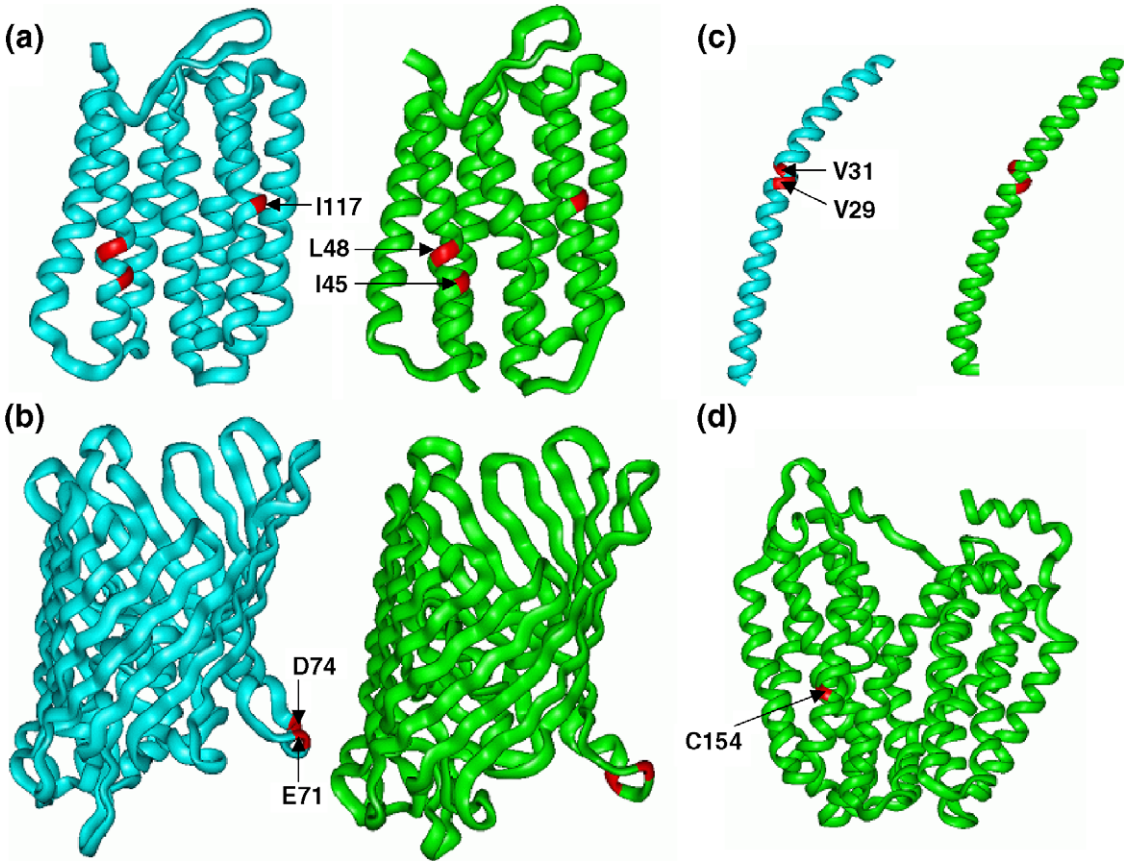

Fig. 3. Comparative views of the protein structures obtained from comparative modeling (cyan) and the X-ray structures (green); (a) bacteriorhodopsin, (b) OmpF porin, and (c) M13 coat protein. For lactose permease (d), the X-ray structure is used in SFE calculation. The positions of mutated residues are shown in red.

of 10 Å. As an estimate of the statistical error, we used half the difference in absolute values between the forward and reverse free energy changes, and the error in $\Delta\Delta G_{sol}$ is calculated as the square root of the sum of the squares of the individual errors in ΔG_{aq} and ΔG_{g}.

3. Results and discussion

Fig. 2 displays the sequence alignments between the targets and their respective templates, which are used in the subsequent comparative modelling. Of the ten structural models calculated for each of the targets, we select the one with the lowest value of the MODELLER objective function as the final structural model of the target protein. The geometries of these final models are then evaluated with PROCHECK [23]. We find that most of the backbone Φ and Ψ dihedral angles are located within the "most favorable" and "additionally allowed" regions in the Ramachandran plots. A few residues are found in the "generously allowed" region, but none are found in the "disallowed" region. These good stereochemical qualities are not surprising, because the sequence identity between the templates and the targets is higher than 60% as illustrated in Fig. 2. Fig. 3 shows the structures of MPs under consideration that are constructed from the comparative modeling as compared with their actual structures determined from X-ray crystallography.

In the case of lactose permease, the X-ray structure is used directly in FEP calculation because neither a homologue for homology modeling nor a remote homologue for the threading by fold recognition is available in the Protein Data Bank. Although bacteriorhodopsin and OmpF porin are oligomeric, only the models of monomeric forms are built because of the lack of a reliable computational method to predict the quaternary structure of an oligomeric protein. Nevertheless, it will be shown that calculating SFE change with the monomer model may be sufficient to explain the mutation-induced change in thermostabilities of the oligomeric MPs.

Fig. 4 shows the time dependence of the root-mean-square deviations of all C_α atoms from starting structures ($RMSD_{init}$) in the $E_1 \rightarrow E_2$ free energy simulations in solution and in the gas phase. In most cases, the $RMSD_{init}$ values remain within 2 Å with a convergent behaviour with respect to the simulation time, indicating the stability of protein structure during the entire course of the free energy simulations [24]. This result is consistent with previous experimental findings from mutagenesis studies, which

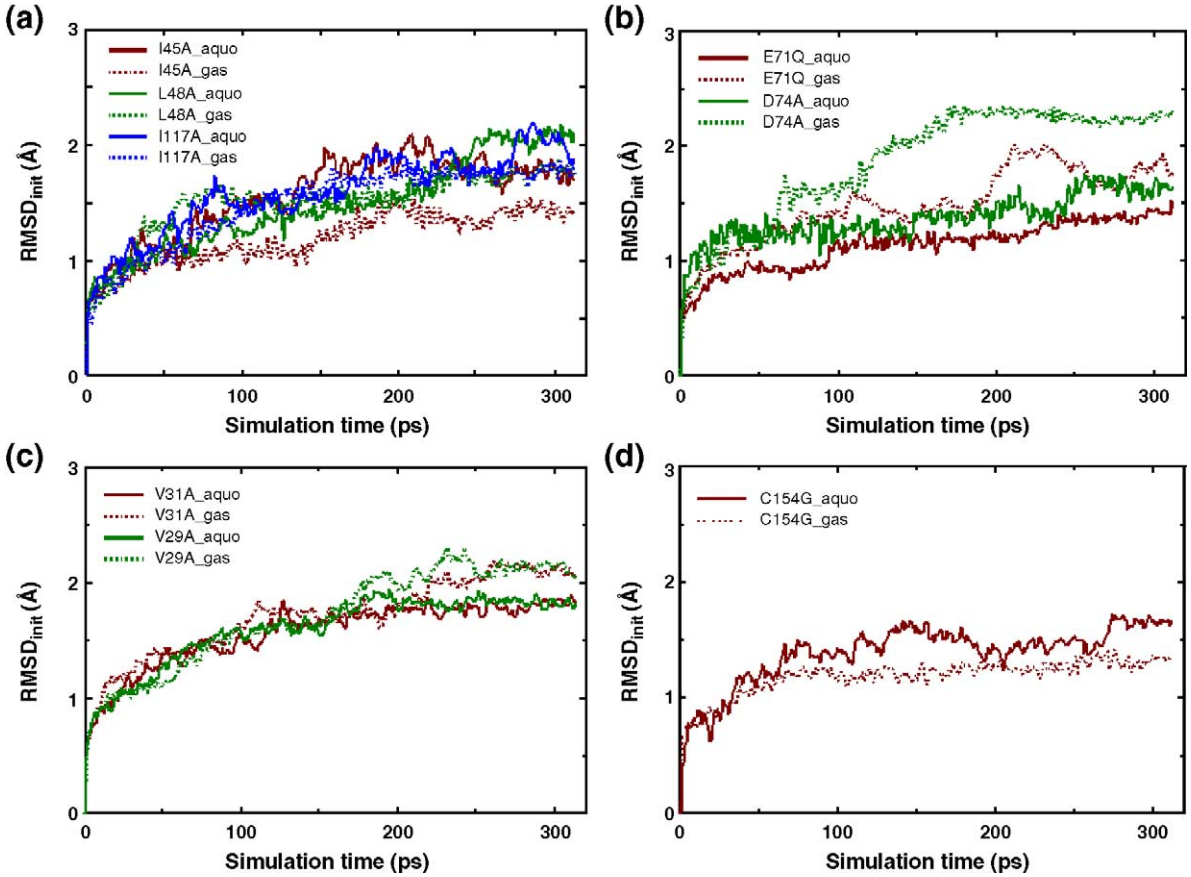

Fig. 4. Time dependence of the root-mean-square deviations from the starting structures for (a) bacteriorhodopsin, (b) OmpF porin, (c) M13 coat protein, and (d) lactose permease.

showed that all the mutations considered in this work did not cause a structural transition at room temperature [6,7,10,12]. In the simulations of I117A in solution, E71G and D74A in the gas phase, the $RMSD_{init}$ plot look less stable than other cases. Therefore, we calculate 2 ps time average of total energies in free energy simulations for the three cases of mutations to provide evidence for a dynamic stability of the systems under the simulation condition described in the previous section. As shown in Fig. 5, the averaged total energies level off around 100 ps in all three cases and are maintained stable in the later part of the simulations.

To address the dependence of simulation time on the conformational stability, we also calculate the time evolution of $RMSD_{init}$ values for I117A mutation of bacteriorhodopsin for 630 ps of simulation time with 10 ps of equilibration and 20 ps of data collection (see Fig. 6). It is seen that the $RMSD_{init}$ values are maintained around 2 Å in the later part of simulation, further supporting the stability of protein conformation during the free energy simulation.

Although the M13 coat protein is known to exist in both monomeric and dimeric forms, it can be taken as a monomeric MP because the relative population of the dimeric form is low [25]. In contrast, lactose permease is definitely known to exist and function as a monomer [26]. Table 1 lists the calculated values of $\Delta\Delta G_{sol}$ for various mutants of these two monomeric MPs in comparison with the experimentally determined relative thermostabilities of the mutant proteins with respect to WT. It is seen that the V31A and V29A mutants are better solvated than the WT in accordance with their enhanced thermostabilities. We also note that $\Delta\Delta G_{sol}$ of V31A mutant is numerically larger than that of V29A mutant, which is consistent with the higher thermostability of the former than the latter [7]. As in the M13 coat protein case, the C154G mutant of lactose permease with a favorable value of $\Delta\Delta G_{sol}$ is in agreement

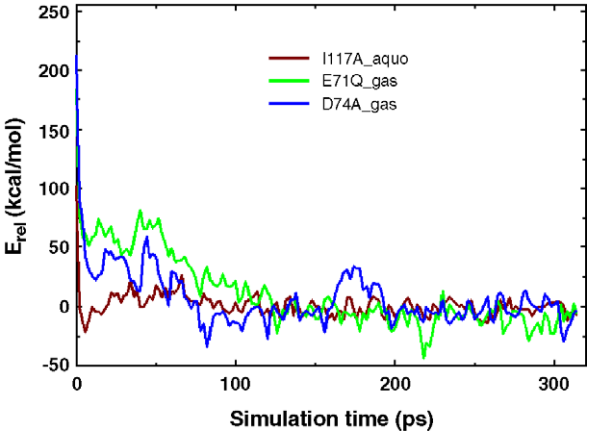

Fig. 5. Variation of 2ps time average of total energies in free energy simulations for the mutations of I117A in solution (brown), E71G in the gas phase (green), and D74A in the gas phase (blue). For comparison, all energy values are measured from the median values in each free energy simulation.

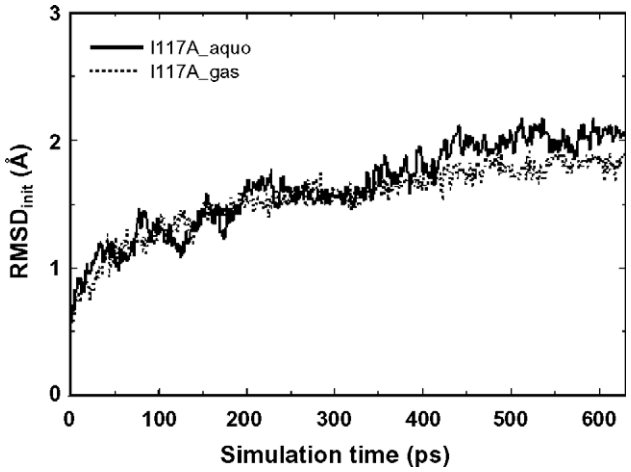

Fig. 6. Time evolutions of the root-mean-square deviations from the starting structures for the free energy simulation for I117A mutant of bacteriorhodopsin in solution (solid line) and in the gas phase (dotted line).

with its higher thermostability than WT in aqueous solution [10]. The FEP calculations also predict that the C154G mutant should be more stable than the WT by 2–3 kcal/mol in aqueous solution as confirmed by the experimental measurement by lipid dilution method [10]. It is thus apparent that in order to obtain mutants of a monomeric MP with an improved thermodynamic stability, the substitution of a residue should be made in such a way that the resulting mutant protein can attain a more negative value of $\Delta\Delta G_{sol}$ relative to the WT.

Summarized in Table 2 are the calculated values of $\Delta\Delta G_{sol}$ for mutants of the two oligomeric MPs in comparison with the experimentally determined relative thermostability with respect to their WTs. It is interesting to note that in contrast to the cases of monomeric MPs, a mutant of oligomeric MP proves to be destabilized as its monomer is stabilized in solution. For example, the order of relative stabilities of the bacteriorhodopsin mutant oligomers (I117A~L48A<WT<I45A) reported by Isenbarger and Krebs [6] is opposite to that for the mutant monomers as indicated by the calculated values of $\Delta\Delta G_{sol}$. This result tells that an oligomeric bacteriorhodopsin with

Table 1
Calculated free energy changes in the gas phase (ΔG_g) and in aqueous solution (ΔG_{aq}), and the SFE change ($\Delta\Delta G_{sol}$) for a transformation of the two WT monomeric MPs to their respective mutants, as compared with the experimentally determined thermostability of a mutant relative to the WT

Mutation	ΔG_g	ΔG_{aq}	$\Delta\Delta G_{sol}$	Thermostability
M13 coat protein				
V31A	−27.5±0.0	−29.2±0.4	−1.6±0.4	↑
V29A	−27.6±0.2	−28.3±0.0	−0.8±0.2	↑
Lactose permease				
C154G	1.5±0.5	−1.2±0.1	−2.6±0.5	↑

All energy values are given in kcal/mol. ↑ and ↓ signs represent the increase and decrease in the thermostability for a given point mutation, respectively.

Table 2
Calculated free energy changes in the gas phase (ΔG_g) and in aqueous solution (ΔG_{aq}), and $\Delta\Delta G_{sol}$ for the transformation of a monomer of the two oligomeric MPs into their various mutants, in comparison with the experimentally determined thermostabilities of oligomeric mutant proteins relative to the WT

Mutation	ΔG_g	ΔG_{aq}	$\Delta\Delta G_{sol}$	Thermostability
Bacteriorhodopsin				
I45A	−15.2±0.2	−13.8±0.4	1.4±0.4	↑
L48A	−4.7±0.4	−7.4±0.8	−2.7±0.9	↓
I117A	−6.7±0.3	−8.3±0.4	−1.6±0.5	↓
	[−7.2±0.1]	[−9.3±0.4]	[−2.1±0.4]	
OmpF porin				
E71Q	−4.3±0.1	−6.2±0.2	−1.9±0.2	↓
	(−4.0±0.1)	(−6.1±0.3)	(−2.1±0.3)	
D74A	7.4±0.5	6.2±0.1	−1.2±0.5	↓
	(7.2±0.5)	(6.2±0.1)	(−1.0±0.5)	

All energy values are given in kcal/mol. ↑ and ↓ signs represent the increase and decrease in the thermostability for a given point mutation, respectively. Numbers in bracket and in parenthesis indicate the free energy values obtained with increased simulation time (10 ps of equilibration and 20 ps of data collection) and with the increased nonbonded-interaction cut-off radius of 12 Å, respectively.

enhanced stability in solution can be derived by a point mutation that reduces the desolvation cost for oligomerization. It is also noteworthy that the $\Delta\Delta G_{sol}$'s for the three single point mutations are different, despite the fact that the changes in the side-chain hydrophobicity are identical or quite similar. This implies that the acquired stability of a mutated monomer in solution stems from complex many-body effects rather than the local increase in the solubility of a single amino acid residue.

Consistent with the results for bacteriorhodopsin, an enhanced solvation in the mutated monomer is found to destabilize the trimeric OmpF porin. Thus the larger increment of SFE in the E71Q mutant monomer than in the D74A mutant monomer accounts for the relative instability of E71Q trimer as compared to the D74A trimer [12]. However, it is rather unexpected that substitutions of the neutral residues for the ionized ones lead to better solvation of the resulting mutant monomers. Since both Glu71 and Asp74 are exposed to the bulk solvent (see Fig. 3), one would expect that both E71Q and D74A mutant monomers are less stabilized in solution than the WT monomer. But this is not the case. It seems that the enhanced solvation in the two mutated monomers is due to the fact that the mutants are destabilized to a larger extent in the gas phase than in aqueous solution. This can be understood by the fact that the contribution of an ionized side chain to the long-range electrostatic interactions is important in the gas phase, but is relatively insignificant in solution due to a strong screening [27].

Considering the importance of long-range electrostatic interactions in free energy simulations especially in a charged system, we carried out another FEP calculation for the E71Q and D74A mutants of OmpF porin with the increased nonbonded-interaction cut-off radius of 12 Å. As shown in Table 2, the results for solution-phase simulations seem not to be influenced significantly by the increase of the cut-off distance. However, the calculated free energy values undergo 0.2–0.3 kcal/mol change in the gas phase simulations, further supporting a greater importance of long-range electrostatic interaction in the gas phase than in solution.

The mutation-induced change in the desolvation cost for trimerization of OmpF porin is estimated to be 3–6 kcal/mol in this study, which is insufficient to explain the experimentally measured destabilization (>10 kcal/mol) of the trimeric mutants [12]. Such a discrepancy indicates that the change in monomer solvation due to a point mutation is not the only contributor to the thermostability of the OmpF porin trimer. Nevertheless, judging from the consistency in reproducing the rank orders of thermostability in the two cases of oligomeric MPs, it is apparent that the calculated $\Delta\Delta G_{sol}$ of a mutant monomer can serve as a reasonable estimate of the relative stability of the corresponding oligomeric MP mutant in solution.

4. Conclusions

By means of a combined computational protocol involving comparative protein structure modeling and free energy perturbation simulation, we have found that the mutation-induced change in solvation free energy would be a useful indicator for finding stability-enhancing mutations for both monomeric and oligomeric MPs in aqueous solution. The utility of the computational strategy is proved by predicting the rank orders of the thermodynamic stabilities of wild type and mutant MPs for bacteriorhodopsin, OmpF porin, M13 coat protein, and lactose permease. A mutant is found to be more stable than WT if the calculated SFE indicates a favorable change for monomeric MPs, whereas for oligomeric MPs the stability of a mutant increases as the mutated monomer is destabilized in solution. This implies that the oligomeric MP mutant can be stabilized in solution due to the reduced desolvation cost for oligomerization. Further study is needed to find additional factors contributing to the mutation-induced stabilization of oligomeric MPs.

Acknowledgment

This work was supported by Grant No. R02-2002-000-00006-0 from the Basic Research Program of the Korea Science and Engineering Foundation. The authors would like to acknowledge the support from KISTI (Korea Institute of Science and Technology Information) under "The Sixth Strategic Supercomputing Support Program" with Dr. Min Sun Yeom as the technical supporter. The use of the computing system of the Supercomputing Center is also greatly appreciated.

References

[1] Y. Kyogoku, Y. Fujiyoshi, I. Shimada, H. Nakamura, T. Tsukihara, H. Akutsu, T. Odahara, T. Okada, N. Nomura, Structural genomics of membrane proteins, Acc. Chem. Res. 36 (2003) 199–206.

[2] P.L. Yeagle, A.G. Lee, Membrane protein structure, Biochim. Biophys. Acta 1565 (2002) 143.

[3] M. Roth, A. Lewit-Bentley, H. Michel, J. Deisenhofer, R. Huber, D. Oesterhelt, Detergent structure in crystals of a bacterial photosynthetic reaction center, Nature 340 (1989) 659–662.

[4] C. Tribet, R. Audebert, J.-L. Popot, Amphipols: polymers that keep membrane proteins soluble in aqueous solutions, Proc. Natl. Acad. Sci. U. S. A. 93 (1996) 15047–15050.

[5] J.U. Bowie, Stabilizing membrane proteins, Curr. Opin. Struct. Biol. 11 (2001) 397–402.

[6] T.A. Isenbarger, M.P. Krebs, Thermodynamic stability of the bacteriorhodopsin lattice as measured by lipid dilution, Biochemistry 40 (2001) 11923–11931.

[7] C.M. Deber, A.R. Khan, Z. Li, C. Joensson, M. Glibowicka, J. Wang, Val→Ala mutations selectively alter helix–helix packing in the transmembrane segment of phage M13 coat protein, Proc. Natl. Acad. Sci. U. S. A. 90 (1993) 11648–11652.

[8] E. Perozo, D.M. Cortes, L.G. Cuello, Three-dimensional architecture and gating mechanism of a K^+ channel studied by EPR spectroscopy, Nat. Struct. Biol. 5 (1998) 459–469.

[9] F.W. Lau, S. Nauli, Y. Zhou, J.U. Bowie, Changing single side-chains can greatly enhance the resistance of a membrane protein to irreversible inactivation, J. Mol. Biol. 290 (1999) 559–564.

[10] I.N. Smirnova, H.R. Kaback, A mutation in the lactose permease of *Escherichia coli* that decreases conformational flexibility and increases protein stability, Biochemistry 42 (2003) 3025–3031.

[11] H. Luecke, B. Schobert, H.-T. Richter, J.-P. Cartailler, J.K. Lanyi, Structural changes in bacteriorhodopsin during ion transport at 2 angstrom resolution, Science 286 (1999) 255–260.

[12] P.S. Phale, A. Philippsen, T. Kiefhaber, R. Koebnik, V.P. Phale, T. Schirmer, J.P. Rosenbusch, Stability of trimeric OmpF porin: the contributions of the latching loop L2, Biochemistry 37 (1998) 15663–15670.

[13] D.A. Marvin, R.D. Hale, C. Nave, M.H. Citterich, Molecular models and structural comparisons of native and mutant class I filamentous bacteriophages Ef (fd, f1, M13), IF1 and Ike, J. Mol. Biol. 235 (1994) 260–286.

[14] J. Abramson, J.I. Smirnova, V. Kasho, G. Verner, H.R. Kaback, S. Iwata, Structure and mechanism of the lactose permease of *Escherichia coli*, Science 301 (2003) 610–615.

[15] J.D. Thompson, D.G. Higgins, T.J. Gibson, CLUSTAL W: improving the sensitivity of progressive multiple sequence alignment through sequence weighting, position-specific gap penalties and weight matrix choice, Nucleic Acids Res. 22 (1994) 4673–4680.

[16] N. Enami, H. Okumua, T. Kouyama, X-ray crystallographic studies of archaerhodopsin, J. Photosci. 9 (2003) 320–322.

[17] S.W. Cowan, T. Schirmer, G. Rummel, M. Steiert, R. Ghosh, R.A. Pauptit, J.N. Jansonius, J.P. Rosenbusch, Crystal structures explain functional properties of two *E. coli* porins, Nature 358 (1992) 727–733.

[18] A. Sali, T.L. Blundell, Comparative protein modelling by satisfaction of spatial restraints, J. Mol. Biol. 234 (1993) 779–815.

[19] D.A. Case, D.A. Pearlman, J.W. Caldwell, T.E. Cheatham III, W.S. Ross, C. Simmerling, T. Darden, K.M. Merz Jr., R.V. Stanton, A. Cheng, J.J. Vincent, M. Crowley, V. Tsui, R. Radmer, Y. Duan, J. Pitera, I. Massova, G.L. Seibel, U.C. Singh, P. Weiner, P.A. Kollman, AMBER, vol. 7, University of California, San Francisco, 2002.

[20] W.D. Cornell, P. Cieplak, C.I. Bayly, I.R. Gould, K.M. Merz Jr., D.M. Ferguson, D.C. Spellmeyer, T. Fox, J.W. Caldwell, P.A. Kollman, A second generation force field for the simulation of proteins, nucleic acids, and organic molecules, J. Am. Chem. Soc. 117 (1995) 5179–5197.

[21] W.L. Jorgensen, J. Chandrasekhar, J.D. Madura, R.W. Impey, M.L. Klein, Comparison of simple potential functions for simulating liquid water, J. Chem. Phys. 79 (1983) 926–935.

[22] J.P. Ryckaert, G. Ciccotti, H.G. Berendsen, Numerical integration of the cartesian equations of motion of a system with constraints: molecular dynamics of *n*-alkanes, J. Comput. Phys. 23 (1977) 327–341.

[23] R.A. Laskowski, M.W. MacArthur, D.S. Moss, J.M. Thornton, PROCHECK: a program to check the stereochemical quality of protein structures, J. Appl. Crystallogr. 26 (1993) 283–291.

[24] C.E. Capener, M.S.P. Sansom, Molecular dynamics simulations of a K channel model: sensitivity to changes in ions, waters, and membrane environment, J. Phys. Chem., B 106 (2002) 4543–4551.

[25] N.G. Haigh, R.E. Webster, The major coat protein of filamentous bacteriophage f1 specifically pairs in the bacterial cytoplasmic membrane, J. Mol. Biol. 279 (1998) 19–29.

[26] L. Guan, F.D. Murphy, H.R. Kaback, Surface-exposed positions in the transmembrane helices of the lactose permease of *Escherichia coli* determined by intermolecular thiol cross-linking, Proc. Natl. Acad. Sci. U. S. A. 99 (2002) 3475–3480.

[27] E.T. Johnson, W.W. Parson, Electrostatic interactions in an integral membrane protein, Biochemistry 41 (2002) 6483–6494.